NJC

Accepted Manuscript

This is an *Accepted Manuscript*, which has been through the Royal Society of Chemistry peer review process and has been accepted for publication.

Accepted Manuscripts are published online shortly after acceptance, before technical editing, formatting and proof reading. Using this free service, authors can make their results available to the community, in citable form, before we publish the edited article. We will replace this *Accepted Manuscript* with the edited and formatted *Advance Article* as soon as it is available.

You can find more information about *Accepted Manuscripts* in the **Information for Authors**.

Please note that technical editing may introduce minor changes to the text and/or graphics, which may alter content. The journal's standard **Terms & Conditions** and the **Ethical guidelines** still apply. In no event shall the Royal Society of Chemistry be held responsible for any errors or omissions in this *Accepted Manuscript* or any consequences arising from the use of any information it contains.

www.rsc.org/njc

ARTICLE TYPE

Catalytic activity of MnO$_x$/WO$_3$ nanoparticles: Synthesis, structure characterization and Oxidative degradation of methylene blue

Mojtaba Amini*[a], Behzad Pourbadiei[a], T. Purnima A. Ruberu [b] and L. Keith Woo[b]

5

MnO$_x$/ WO$_3$ nanoparticles were synthesized by an impregnation method and the physicochemical properties of compounds were characterized by atomic absorption spectroscopy (AAS), energy dispersive X-ray analysis (EDX), X-ray diffraction (XRD), scanning
10 electron microscopy (SEM) and transmission electron microscopy (TEM). The catalytic degradation of an organic dye, methylene blue, in the presence of nano-MnOx supported on WO$_3$ as catalyst and hydrogen peroxide, H$_2$O$_2$, as the oxidant has been studied at room temperature in water. Effects of oxidant amount, catalyst composition and an OH-radical scavenging agent on the degree of decomposition of MB dye were also studied.

.
15

Introduction

Methylene blue (MB) is one of the most commonly used dyes in various industries for textiles, printing, rubber, etc. [1-3]. The effluents from these industries are a major source of
20 environmental pollution. Not only do water bodies become colored, but environmental damage occurs to living organisms by decreasing the dissolved oxygen capacity of water and by blocking sunlight, thereby disturbing the natural growth activity of aquatic life. Therefore, the treatment of effluents containing
25 dyes is one of the challenging problems in the field of environmental chemistry [4-8].

The synthesis and characterization of complex transition-metal oxides with controlled size, shape, uniform dimension, and structure have attracted considerable interest due to their unique
30 physicochemical properties and potential applications in catalysis and material science [9–12]. Among these, manganese and tungsten oxides have gained increasing attention because of outstanding structural diversity and useful chemical and physical properties, which makes them suitable for various applications
35 such as catalysis, water treatment, lithium-ion batteries, magnetic resonance imaging, sensor material, etc. [9–16]. These compounds are cheap, environmentally friendly and can be prepared as nano-sized particles with large surface area, with high active sites densities. Their polynuclear structure should allow the
40 occurrence of multi-electron and complex reactions. Moreover, metal oxides have no easily oxidizable ligands and thus are robust under a wide range of conditions. They could be used in bulk, supported, or colloidal forms and can be synthesized easily [17, 18].
45 Among many applications, manganese oxide has been widely used for the degradation of organic dyes for environmental remediation [19–21]. Recently Nie et al. reported layered manganese oxide suspension as a highly effective catalyst for the decolorization and degradation of methylene blue in the presence
50 of H$_2$O$_2$ at neutral pH [22]. Also, other studies [23, 24]

investigated the use of manganese oxides to degrade organic pollutants.

Herein we report the first preparation of nano-MnO$_x$ supported on WO$_3$ as an efficient catalyst for the green decomposition of
55 methylene blue (MB) using hydrogen peroxide (H$_2$O$_2$) as the oxidant (Scheme 1). The extent of dye decomposition was monitored using UV-vis spectroscopic techniques.
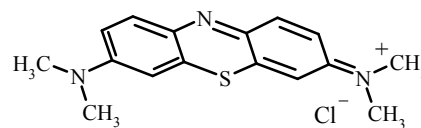
60 Scheme 1. Structure of methylene blue (MB).

Experimental

Materials

Characterization

Transmission electron microscopy (TEM) was conducted on carbon-coated copper grids using a FEI Technai G2 F20 Field
70 Emission scanning transmission electron microscope (STEM) at 200 kV (point-to-point resolution <0.25 nm, line-to-line resolution <0.10 nm). TEM samples were prepared by placing 2-3 drops of dilute ethanol solutions of the nanomaterials onto carbon coated copper grids. Composition was characterized by
75 energy dispersive spectroscopy (EDS) line scans in STEM mode, and by energy-filtered (EF) imaging spectroscopy (EF-TEM).
SEM was carried out with Philips CM120 and LEO 1430VP instruments. The X-ray powder patterns were recorded with a Bruker D8 ADVANCE (Germany) diffractometer (Cu-Kα

radiation). Manganese content in bulk and on the catalyst surface was determined by atomic absorption spectroscopy (AAS) and energy-dispersive X-ray (EDX). AAS was performed on a Varian Atomic Absorbtion Spectrometer AA 110. Prior to analysis, the

5 oxide (1.0 mg) was added to 1 mL of concentrated nitric acid and H_2O_2, left at room temperature for at least 2 h to ensure that the oxides were completely dissolved. The solution was then diluted to 10.0 mL and analyzed by AAS. Absorption spectra were recorded by a CARY 100 Bio VARIAN UV–vis

10 spectrophotometer. FT-IR spectrum was obtained by using a Unicam Matson 1000 FT-IR spectrophotometer using KBr disks at room temperature.

Synthesis

15 An aqueous solution (10 cm³) of $Na_2WO_4 \cdot 2H_2O$ (0.825 g; 2.5 mmol) was acidified with a HCl solution (6 M), and a white precipitate of $WO_3 \cdot nH_2O$ was obtained. The solid of $WO_3 \cdot nH_2O$ was washed with water for several times and dried at 50 °C. WO_3 was prepared by dehydration of $WO_3 \cdot nH_2O$ at 500 °C for 3h.

20 MnO_x supported on WO_3 was prepared by an impregnation method using $Mn(NO_3)_2 \cdot 4H_2O$ as a source for Mn. The required amount of $Mn(NO_3)_2 \cdot 4H_2O$, to give 5 wt% Mn loading, was mixed and was pulverized with WO_3. Methanol (20 mL) was added to the mixture of $Mn(NO_3)_2$ and WO_3. This mixture was

25 mechanically stirred to ensure the homogeneous distribution of $Mn(NO_3)_2 \cdot 4H_2O$ over the WO_3 support. After stirring, CH_3OH was evaporated under vacuum using a rotary evaporator. Dissolution of $Mn(NO_3)_2 \cdot 4H_2O$ and evaporation of CH_3OH were performed three times to optimize the distribution of

30 $Mn(NO_3)_2 \cdot 4H_2O$. After the third evaporation process, the residual solid was ground and calcinated at 500 °C for 4h. MnO_x was prepared by taking an aqueous solution of $Mn(NO_3)_2 \cdot 4H_2O$ and urea as a fuel in a muffle furnace maintained at 500 °C for 4h.

35

Methylene blue degradation

The catalytic activity of the catalyst was demonstrated by degrading MB in aqueous solution. A round-bottom flask was charged with 50 mL of aqueous MB (10 mg/L) and 10 mg of

40 catalyst was added. H_2O_2, (10 mL, 0.1 mol) was added and the reaction mixture and was stirred under ambient conditions. For a given time interval, a small quantity of the mixture solution was pipetted into a quartz cell, and its absorption spectrum was measured using an UV–visible spectrophotometer.

45

Results and Discussion

Catalyst characterization

The X-ray powder diffraction patterns of MnO_x/WO_3 catalyst are

50 shown in Fig. 1. Data for pure WO_3 are also included in Fig. 1. The XRD pattern of the WO_3 support contains peaks corresponding to lattice reflection planes (002), (020), (200), (120), (112), (112), (201), (220), (222), (004), (040), (140), (420), and (402) as referred in the JC-PDS 01-075-2072 [25]. As shown

55 Fig. 1, the manganese oxide pattern was difficult to estimate from the XRD data, due to the fact that the most intense lines of the manganese oxide phase almost coincide with the diffraction lines of the WO_3 support.

However, the support line intensity decreased with the loading of

60 manganese on the WO_3, attributed to the formation of crystalline

manganese oxide. The absence of the XRD peaks of individual MnO_x suggests that the manganese oxide particles are in a highly dispersed state, or that insertion of manganese ions into the WO_3 lattice may occur [26].

65
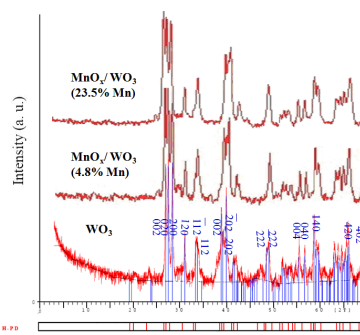
Fig. 1. XRD pattern of WO_3 and MnO_x/WO_3

The amount of the manganese supported on the WO_3 was

70 determined by AAS analysis. The catalyst was stirred in HNO_3 at room temperature for 5 h and the solution was subjected to AAS analysis. MnO_x/WO_3 contained 4.8 wt. % Mn. It is well known that EDX technique supplies an accurate determination of relative atomic concentration of different elements present on their

75 outermost surface layers. EDX investigation of MnO_x/WO_3 showed that the relative atomic abundance of manganese present in the surface of the WO_3 was obtained 3.2% (Table 1). The differences attained for Mn contents in bulk and on the surface of catalyst suggest that the composition of the surface layers of the

80 catalyst is slightly different from its bulk composition.

Table 1. EDX investigation of MnO_x/WO_3

Element	Weight%	Atomic%	correction	k-Factor	Area Scan
O(K)	18.27	71.9	0.49	1.974	
Mn(L)	0.13	0.15	0.57	4.328	
W(L)	81.59	27.94	0.75	5.15	
O(K)	8.66	49.89	0.49	1.974	
Mn(L)	3.68	6.18	0.57	4.328	
W(L)	87.65	43.92	0.75	5.15	

85 The Mn distribution on WO_3, particle morphology and textural properties of MnO_x/WO_3 catalyst was also studied carefully by SEM and TEM and representative images are shown respectively in Fig. 2. and Fig. 3. Aggregated nanoparticles with spherical shapes are observed with particle diameter in the range of 50–80

90 nm.
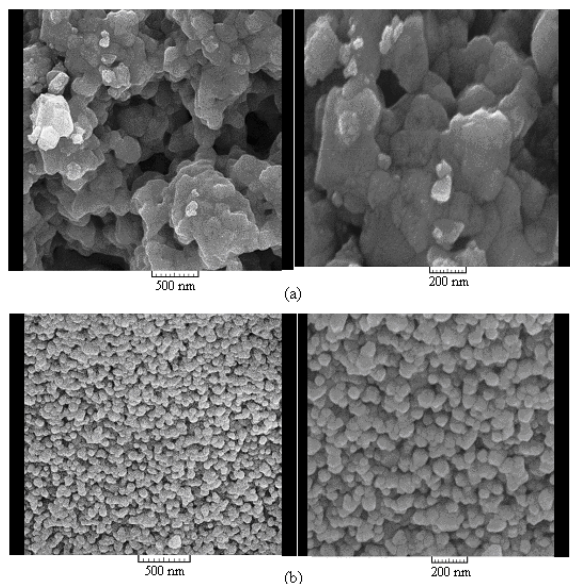
Fig. 2. SEM images of (a) WO₃ (b) MnOₓ/ WO₃
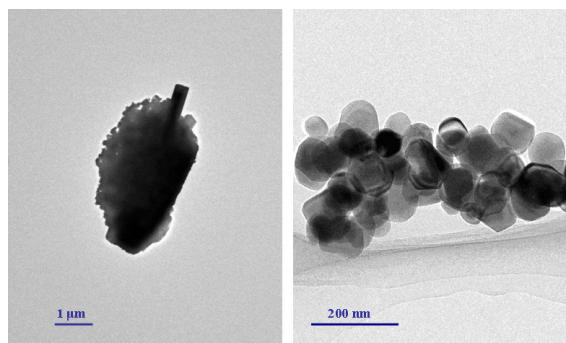
5　　　　Fig. 3. TEM images of MnOₓ/ WO₃

Catalytic effects

10 The activity of the catalysts is expressed as the percent decrease in dye concentration during the reaction, as measured by absorption intensity. A plot of the percentage decrease in [MB] versus time represents the influence of oxidant on the decomposition of MB dye catalyzed by MnOₓ/WO₃ and WO₃
15 alone at room temperature (Fig. 4). As can be seen, nearly no degradation was observed over 120 min, when H₂O₂ alone was added to the MB solution.
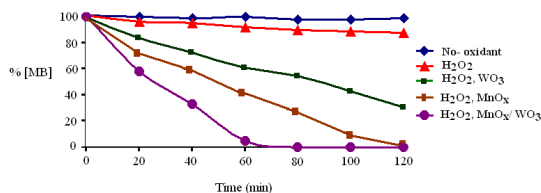
20 Fig. 4. Percentage decomposition of MB with different conditions. The reactions were run in duplicate**.**

The use of different oxides such as Al₂O₃, SiO₂, CeO₂, ZnO and WO₃ as catalyst supports, were also examined to study the effects
25 of support on the catalytic degradation of methylene blue (Fig. 5). When the MnOₓ/WO₃ catalyst was added to the MB solution containing H₂O₂, the removal of MB was complete after 60 min,

showing that MnOₓ/WO₃ facilitated the oxidation of MB by H₂O₂. The catalytic activity of the system decreased dramatically
30 when MnOₓ/WO₃ was replaced by WO₃, as shown in Fig. 4. These results indicate that the absence of MnOₓ substantially increased the decomposition of the dye, because doping process results in changing the chemistry of the surface of treated solids, brings about some changes in the electronic structure of the
35 doped catalysts and may also affect solid–solid interactions between the manganese oxide catalyst and its WO₃ support [27].
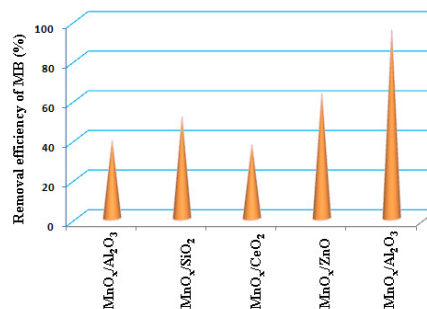
Fig.5. Effects of the catalyst supports on the percentage decomposition of MB. 10mg catalyst, 50 mL MB(10mgL⁻¹), 10mL H₂O₂ (30%); 60 min.
40

The effect of H₂O₂ amount on the percentage decomposition of MB is shown in Fig. 6. When the amount of H₂O₂ varies from 0 to 0.1 mol, the percentage decomposition of MB increased from 0 to ca. 95%. With a further increase of H₂O₂ to 0.15 mol, the time
45 for complete decomposition of MB decreases from 60 to 45 min.
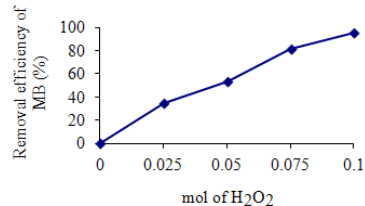
Fig. 6. Effects of the amount of H₂O₂ on the percentage decomposition of MB. 10mg catalyst, 50 mL MB(10mgL⁻¹) ; 60 min.

50 Representative UV–vis spectra changes observed during MB degradation by MnOₓ/WO₃ and WO₃ in the presence of H₂O₂ are depicted in Fig. 7. The intense absorbance of MB at 296 and 664nm decreased rapidly and disappeared almost completely within 60 min in the presence of catalytic MnOₓ/WO₃. When
55 pure WO₃ was used as catalyst, loss of MB took more than 130 min (Fig 7. (b)).

(a)

(b)
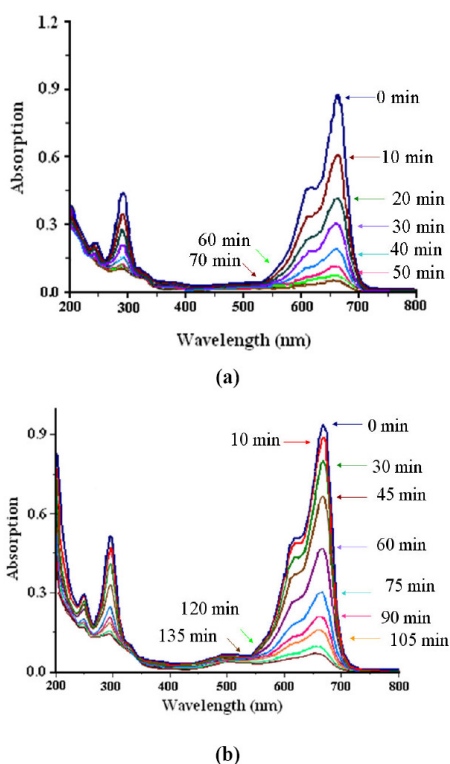
Fig. 7. Changes in the UV-vis absorbance spectra of MB dye using a) MnO_x/WO_3 b) WO_3 catalyst with H_2O_2.

5 The typical IR spectra in region $4000–500cm^{-1}$ of MB before and after treatment also demonstrated the total degeneration of dye (Fig. 8).The IR spectra of MB exhibit C=N and C–N stretching vibration peaks in the heterocycle of MB at 1604 and $1399cm^{-1}$, respectively and the C–N bond connected with benzene ring and

10 N–CH3 at 1356 and $1332cm^{-1}$ [28]. After treating dye by air for about 60 min, these peaks decrease in intensity to disappear, indicating the total destruction of aromatic ring of dye molecule in the presence of MnO_x/WO_3 catalyst and H_2O_2.
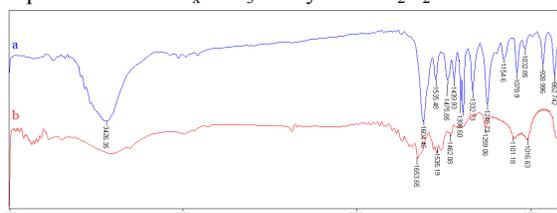
15 Fig. 8. Changes of MB in FT-IR spectra during degradation: (a) 0 min; (b) after 60 min reaction

In order to show the merit and efficiency of the present catalytic system in comparison with recently reported protocols, we

20 compared the results of the MB removal in the presence of other catalysts. As shown in Table 2, our catalytic system is superior to some of the previously reported catalysts in terms of reaction conditions. In contrast to similar, previously reported systems, the catalytic system presented in this paper does not suffer from the

25 harsh reaction conditions, such as high calcination temperature (entry 2), long reaction time (entries 2-5), using large amount of catalyst (entries 3, 4) and using large amounts of oxidant (entry 5). In addition, the attractive features of this catalytic system, such as low cost, and ease of use, make it particularly suitable for

30 the MB removal.

Table 2. Recently reported catalytic systems for the MB removal by different catalysts.

Entry	Catalyst	MB removal Conditions	Catalyst preparation conditions	Ref.
1	MnO_x/WO_3	10mg catalyst, 50 mL $MB(10mgL^{-1})$, 10mL H_2O_2; 60 min.	Calcinated at 500 °C	Present work
2	Nanorods of manganese oxides	10mg catalyst, 50 mL $MB(10mgL^{-1})$, 10mL H_2O_2; 160 min.	Calcinated at 500-800 °C under N_2	[23]
3	TiO2–Mn oxide	25mg catalyst, 50 mL $MB(10mgL^{-1})$, 1.5mL H_2O_2; 120 min.	Calcinated at 500 °C	[24]
4	iron oxide/activated carbon	30mg catalyst, 7 mL $MB(500mgL^{-1})$, 7mL H_2O_2; 25h.	Calcinated at 300 °C	[29]
5	layered manganese oxide	10mg catalyst, 50 mL $MB(30mgL^{-1})$, 55mL H_2O_2; 100 min.	No need to calcination	[22]

35

It has been reported that the catalytic removal of methylene blue in the presence of H_2O_2 and manganese oxide follows a radical oxidation pathway [30]. This pathway may be taken due to hydrogen peroxide being a source of OH radicals when

40 decomposed homolytically. Therefore, to further verify the role of OH radicals in the oxidation system of the nano-MnO_x supported on WO_3, we examined the effects of DMSO as an OH-radical scavenging agent in this process. The hydroxyl radicals could react with DMSO to give high yields of CH3 radicals,

45 which leads to methane and ethane as final products [31]. As shown in Fig. 9, the removal of MB was decreased from 95% to 64% in the presence of DMSO within 60 min. This suppressive effect was dependent on the concentration of DMSO under these conditions. These results confirmed that OH radicals have the

50 main role in the decolorizing process, which is enhanced by H_2O_2 and suppressed by DMSO.
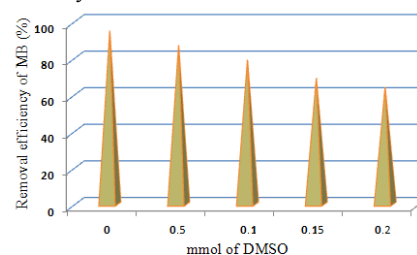
Fig. 9. Effects of various concentrations of DMSO on the removal of methylene blue in the presence of MnO_x/WO_3 and H_2O_2. 10mg catalyst,

55 50 mL $MB(10mgL^{-1})$, 10mL H_2O_2 (30%); 60 min.

In order to clarify the role of manganese in the product of hydroxyl radicals, new catalyst of MnO_x/WO_3 with 23.5% Mn loading were prepared. As shown Fig.1, the X-ray powder

60 diffraction patterns of MnO_x/WO_3 (23.5% Mn) showed no significant change with the XRD pattern of the MnO_x/WO_3 (4.8% Mn). Also the result of catalytic studies reveals that two MnO_x/WO_3 catalysts with different Mn loading are almost equally effective in catalysis of the MB degradation. Therefore,

65 manganese is not only effective for the product of OH radicals and WO_3 as support have also essential role.

Finally, the effect of repeated uses of the catalyst on its catalytic activity was examined. After the end of the first experiment, the catalyst was washed with doubly distilled water, and dried prior

70 to the next use. The results in Fig. 10 demonstrated that MnO_x/WO_3 maintained similar activity after a four runs of the catalyst.
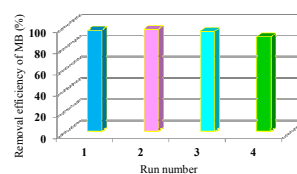
Fig. 10. Recycling studies of the MnOx/WO3 catalyst in the degradation of MB. 10mg catalyst, 50 mL MB(10mgL^{-1}), 10mL H$_2$O$_2$ (30%); 60 min.

We also found that XRD and reflectance infrared Fourier transform spectra of both fresh and used catalysts are very similar (Fig. 11). The results show that the catalyst is not changed in the reaction.

(a)   (b)
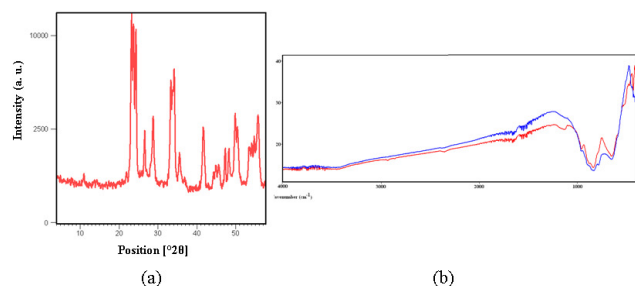
Fig. 11. (a) XRD pattern of used catalyst; (b) IR spectra of fresh (red) and used (blue) catalyst.

Conclusions

The nano-MnO$_x$ supported on WO$_3$ was successfully synthesized using an impregnation method. This new material, MnO$_x$/WO$_3$, was found to be an effective catalyst for the destruction of MB, an important industrial dye and problematic pollutant. Effects of oxidant amount and catalyst composition (WO$_3$ with and without MnO$_x$) on the degree of decomposition of MB dye were also studied. The catalytic activity of the system decreased dramatically when MnO$_x$/WO$_3$ was replaced by WO$_3$. To verify the role of OH radicals in the oxidation system of the nano-MnO$_x$ supported on WO$_3$, the effects of DMSO as an OH-radical scavenging agent was examined in this process. Finally, a further set of experiment was carried out to check the reusability of the MnO$_x$/ WO$_3$ catalyst for the MB degradation at room temperature for 60 min.

Acknowledgments

Notes and references

^{a}Department of Chemistry, Faculty of Science, University of Maragheh, Golshahr, P.O. Box. 55181-83111731, Maragheh, Iran
^{b}Chemistry Department, Iowa State University, Ames, Iowa 50011-3111, USA.

1   P. Bautista, A. F. Mohedano, J. A. Casas, J.A. Zazo and J. J. Rodriguez, *J. Chem. Technol. Biotechnol*. 2008, **83**, 1323.
2   A. Xu, X. Li, S. Ye, G. Yin and Q. Zeng, *Appl. Catal. B: Environ*. 2011, **102**, 37.
3   S. Caudo, G. Centi, C. Genovese and S. Perathoner, *Top. Catal*. 2006, **40**, 207.
4   A. Chithambararaj, N. S. Sanjini, A. Chandra Bose and S. Velmathi, *Catal. Sci. Technol.*, 2013, **3**, 1405.
5   J. M. Monteagudo, A. Durán and C. López-Almodóvar, *Appl. Catal. B* 2008, **83**, 46.
6   A. H. Xu, H. Xiong and G. C. Yin, *J. Phys. Chem. A* 2009, **113**, 12243.
7   H. A. Le, L. T. Linh, S. Chin and J. Jurng, *Powder Tech*., 2012, **225**, 167.
8   O. Impart, A. Katafias, P. Kita, A. Mills, A. Pietkiewicz-Graczyk and G. Wrzeszcz, *Dalton Trans*. 2003, **2003**, 348.
9   J. Cao, Y.Zhu, L.Shi, L.Zhu, K.Bao, S.Liu and Y.Qian, *Eur. J. Inorg. Chem*. 2010, **2010**, 1172.
10   J. Zhao, Z. Tao, J. Liang and J. Chen, Cryst. *Growth Des*. 2008, **8**, 2799.
11   T. Yu, J. Moon, J. Park, Y. I. Park, H. B. Na, B. H. Kim, I. C. Song, W.K. Moon and T. Hyeon, *Chem. Mater*. 2009, **21**, 2272.
12   Y. Ding, C. Hou, B. Li and Y. Lei, *Electroanalysis*, 2011, **23**, 1245.
13   Z.-R. Tian, W. Tong, J.-Y. Wang, N.-G. Duan, V.V. Krishnan and S.L. Suib, *Science* 1997, **276**, 926.
14   C. E. Clarke, F. Kielar, K. L. Johnson, *J. Hazard. Mater*. 2013, **246–247**, 310.
15   M.A. Gondal, A. Bagabas, A. Dastageer and A. Khalil, J. *Mol. Catal. A: Chem*., 2010, **323**, 78.
16   J. Cao, B. Luo, H. Lin and S. Chen, *J. Hazard. Mat*. 2011, **190**, 700.
17   M.M. Najafpour, F. Rahimi, M. Amini, S. Nayeri, M. Bagherzadeh, *Dalton Trans*., 2012, **41**, 11026.
18   M. Amini, M. M. Najafpour, S. Nayeri, B. Pashaei, M. Bagherzadeh, *RSC Adv*., 2012, **2**, 3654.
19   J. Fei, Y. Cui, X. Yan, W. Qi, Y. Yang, K. Wang, Q. He and J. Li, *Adv. Mater*. 2008, **20**, 452.
20   C.E. Clarke, F. Kielar, H. M. Talbot and K.L. Johnson, *Environ*. Sci. Technol. 2010, **44**, 1116.
21   H. Chen, P.K. Chu, J.He, T.Hu and M.Yang, *J. Colloid Interface Sci*. 2011, **359**, 68.
22   L. Zhang, Y. Nie, C. Hu and X. Hu, *J. Hazard. Mater*., 2011, **190**, 780.
23   Z. Yang, Y. Zhang, W. Zhang, X. Wang, Y. Qian, X. Wen and S. Yang, *J. Solid State. Chem*. 2006, **179**, 679.
24   J-H. Park, I. Jang, K. Song and S-G. Oh, *J. Phys. Chem. Solids*, 2013, http://dx.doi.org/10.1016/j.jpcs.2013.03.006i.
25   A. Hemati, M. Allaf B, M. Ranjbar, P. Kameli and H. Salamati, Sol. Energ. Mat. Sol. C., 2013, **108**,105.
26   Y. Wu, S. Liu, H. Wang, X. Wang, X. Zhang and G. Jin, *Electrochim. Acta*, 2013, **90**, 210.
27   L.M. Gandia, M.A.Vicente and A. Gil, *Appl. Catal. B: Environ*. 2002, **38**, 295-307.
28   K. Imamura, E. Ikeda, T. Nagayasu, T. Sakiyama and K. Nakanishi, *J. Colloid Interface Sci*. 2002, **245**, 50.
29   C.S. Castro, M.C. Guerreiro, L.C.A. Oliveira, M. Gonçalves, A.S. Anastácio and M. Nazzarro, *Appl. Catal. A: Gen*. 2009, **367**, 53.
30   S-H. Do, B. Batchelor, H-K. Lee and S-H. Kong, *Chemosphere*, 2009, **75**, 8.
31   M.K. Eberhardt, R. Colina, *J. Org. Chem*. 1988, **53**, 1071.